

Vibration analysis of a shear deformed anti-symmetric angle-ply conical shells with varying sinusoidal thickness

Saira Javed^{1,2}, K.K. Viswanathan^{*1,2}, Z.A. Aziz^{1,2} and J.H. Lee³

¹UTM Centre for Industrial and Applied Mathematics (UTM-CIAM), Ibnu Sina Institute for Scientific & Industrial Research, Universiti Teknologi Malaysia, 81310 Johor Bahru, Johor, Malaysia

²Department of Mathematical Sciences, Faculty of Science, Universiti Teknologi Malaysia, 81310 Johor Bahru, Johor, Malaysia

³Department of Naval Architecture & Ocean Engineering, Division of Mechanical Engineering, Inha University, Incheon 22212, South Korea

(Received April 3, 2015, Revised March 13, 2016, Accepted March 15, 2016)

Abstract. The study is to investigate the free vibration of antisymmetric angle-ply conical shells having non-uniform sinusoidal thickness variation. The arbitrarily varying thickness is considered in the axial direction of the shell. The vibrational behavior of shear deformable conical shells is analyzed for three different support conditions. The coupled differential equations in terms displacement and rotational functions are obtained. These displacement and rotational functions are invariantly approximated using cubic spline. A generalized eigenvalue problem is obtained and solved numerically for an eigenfrequency parameter and an associated eigenvector of spline coefficients. The vibration characteristic of the shells is examined for cone angle, aspect ratio, sinusoidal thickness variation, layer number, stacking sequence, and boundary conditions.

Keywords: vibration; anti-symmetric; conical shell; splines; thickness variation

1. Introduction

The shells of non-uniform thickness are used in ship, rocket, missile and marine industry. The main characteristic of variable thickness shells is to alter frequency, decrease weight, size and ultimately cost of the structure. The composite laminated shell structures have gained interest of engineers during last few decades due to specific properties tailored by suitable arrangement of the stacking sequence of the layers. Moreover, required properties of the structure can be attained by selecting the best aspect of the constituent layers in terms of choice of materials, number of layups, thickness variation of each layer and boundary conditions.

Few researchers worked on anti-symmetric angle-ply structures. Among them the influence of boundary conditions and transverse shear on vibration of angle-ply laminated plates and cylindrical shells was investigated by Soldatos and Messina (2001). Angle-ply laminated conical shells were analysed for their post buckling characteristics by Patel *et al.* (2008). Further,

*Corresponding author, Associate Professor, E-mail: visu20@yahoo.com, viswanathan@utm.my

Viswanathan and Kim (2008) who studied free vibration of anti-symmetric angle-ply plates including shear deformation. Moreover, State space differential quadrature method was used by Alibeigloo (2009) to examine the static and vibration of axi-symmetric angle-ply truncated conical shells. Recently, Qu *et al.* (2013) analysed anti-symmetric angle-ply laminates using unified formulation for vibration analysis of composite laminated shells. Also, Xiang *et al.* (2014) analysed angle-ply and cross ply laminates of conical, cylindrical shells and annular plates structures.

But to the authors knowledge few researchers studied the free vibration of conical shells having variable thickness. Kang (2014) investigated the free vibration of conical shells with linear thickness variation using Ritz method. Selahi *et al.* (2014) analyse the functionally graded truncated conical shells of variable thickness using differential quadrature method and fourier series expansion. Free vibration of ring-stiffened conical shell of variable thickness loading with fluid was analysed by Liu *et al.* (2014). Sofiyev *et al.* (2009) studied the vibration of orthotropic conical shells varying with material properties, in which the variation being along the thickness direction.

Different numerical techniques were used to analyse frequency of plates and shells. Among them Lal and Rani (2014) studied the mode shapes and frequencies of sandwich annular circular plates using differential quadrature method. Modified Fourier series was used to analyse the vibration of conical shells by Jin *et al.* (2014). Dey and Karmakar (2012) investigated the natural frequency of delaminated rotating conical shells using finite element approach. Recently, Chernobryvko (2014) used Ritz method to analyse the free vibration of thin parabolic shells. Akbari *et al.* (2014) analyse free vibration of conical panels consisting of functionally graded materials using differential quadrature method. Haar wavelet method was used to analyse the free vibration of functionally graded conical shells and annular circular plates (Xie 2014). Ansari used a novel variational numerical method for analyzing the free vibration of composite conical shell using Rayleigh-Ritz method. Free and forced vibration of coupled conical-cylindrical shells were analysed using Fourier-Ritz method (Ma *et al.* 2014). Analytical and experimental study of free vibration of joined conical shells was done by Shakouri and Kouchakzadeh (2014). Galerkin and semi inverse method was used by Sofiyev (2014) to analyse the large-amplitude vibration of non-homogeneous composite conical shells. Sofiyev and Kuruoglu (2014) studied the combined influences of shear deformation and rotary inertia on the frequencies of cross-ply laminated orthotropic cylindrical shells. Su *et al.* (2014) studied the three-dimensional vibration analysis of thick functionally graded conical, cylindrical shell and annular plate structures using Fourier series.

Firouz-Abadi (2014) higher order Shear deformation theory was used to analyse thick conical shells using Forbenius method. Further, Higher-order equivalent single layer theories were used by Tornabene *et al.* (2014) to investigate free vibration of doubly-curved shells. Moreover, stress and strain recovery for doubly-curved sandwich shells were investigated using higher-order equivalent single layer theory (Tornabene *et al.* 2014).

Wu *et al.* (2015) used domain decomposition method to study free vibration of conical shell resting on Pasternak foundation. In addition to that, Zarouni *et al.* (2014) analysed the free vibration of fiber reinforced composite conical shells resting on Pasternak-type elastic foundation using Ritz and Galerkin methods. Zhang *et al.* (2015) analysed free vibration analysis of four-unknown shear deformable functionally graded cylindrical micro shells based on the strain gradient elasticity theory. Buckling of heterogeneous orthotropic composite conical shells under external pressures with shear theory has been studied by Sofiyev (2016). In his work the equation

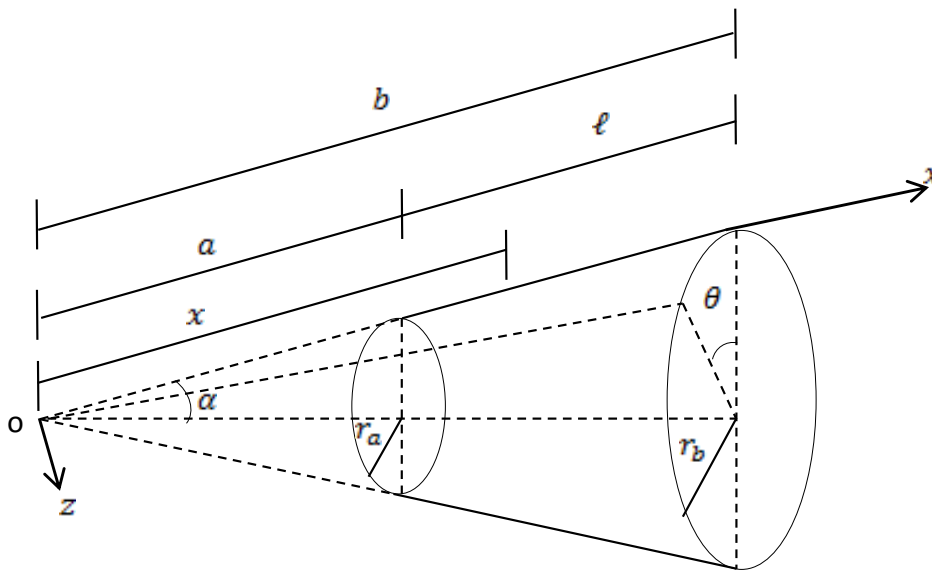


Fig. 1 Coordinate system and geometry of truncated conical shell

of conical shells were derived using Donnell shell theory and approximated using Galerkin’s method.

This paper aims to investigate the free vibration of anti-symmetric angle-ply conical shells of non-uniform sinusoidal thickness variation including shear deformation and applying spline approximation technique. The displacement and rotational functions are predicted using cubic spline. Collocation with these splines yields a set of field equations which along with the equations of boundary conditions, reduce to system of homogeneous simultaneous algebraic equations on the assumed spline coefficients. Then the problem is solved using eigensolution technique to obtain the frequency parameter. The eigenvector are the spline coefficients from which the mode shapes can be constructed. The stability of the conical structure is analysed with respect to the cone angle and length ratio in addition to that, the effect of lamination material, lamination scheme and boundary conditions are analysed on the value of frequency parameter. Graphs and tables signify the obtained results.

2. Formulation of the problem

Consider a truncated conical shell of constant thickness shown in Fig. 1. The orthogonal coordinate system (x, θ, z) is fixed at its reference surface, which is taken to be at the middle surface. The radius of the cone at any point along its length is $r = x \sin \alpha$. The radius at the small end of the cone is $r_a = a \sin \alpha$ and the other end is $r_b = b \sin \alpha$. α is the semi-vertex angle and ℓ is the length of the cone along its generator. The thickness variation is assumed along the axial direction is considered as x -axis.

The stress resultants N_{ij} and moment resultants M_{ij} are defined as

$$\left(N_x, N_\theta, N_{x\theta}, Q_x, Q_\theta \right) = \int_z \left(\sigma_x, \sigma_\theta, \tau_{x\theta}, \tau_{xz}, \tau_{\theta z} \right) dz$$

$$(M_x, M_\theta, M_{x\theta}) = \int_z (\sigma_x, \sigma_\theta, \tau_{x\theta}) z dz \tag{1}$$

The stress-strain relations of the k -th layer by neglecting the transverse normal strain and stress, are of the form

$$\begin{pmatrix} \sigma_x^{(k)} \\ \sigma_\theta^{(k)} \\ \tau_{x\theta}^{(k)} \\ \tau_{\theta z}^{(k)} \\ \tau_{xz}^{(k)} \end{pmatrix} = \begin{pmatrix} Q_{11}^{(k)} & Q_{12}^{(k)} & Q_{16}^{(k)} & 0 & 0 \\ Q_{12}^{(k)} & Q_{22}^{(k)} & Q_{26}^{(k)} & 0 & 0 \\ Q_{16}^{(k)} & Q_{26}^{(k)} & Q_{66}^{(k)} & 0 & 0 \\ 0 & 0 & 0 & Q_{44}^{(k)} & Q_{45}^{(k)} \\ 0 & 0 & 0 & Q_{45}^{(k)} & Q_{55}^{(k)} \end{pmatrix} \begin{pmatrix} \epsilon_x^{(k)} \\ \epsilon_\theta^{(k)} \\ \gamma_{x\theta}^{(k)} \\ \gamma_{\theta z}^{(k)} \\ \gamma_{xz}^{(k)} \end{pmatrix} \tag{2}$$

When the materials are oriented at an angle θ with the x -axis, the transformed stress-strain relations are

$$\begin{pmatrix} \sigma_x^{(k)} \\ \sigma_\theta^{(k)} \\ \tau_{x\theta}^{(k)} \\ \tau_{\theta z}^{(k)} \\ \tau_{xz}^{(k)} \end{pmatrix} = \begin{pmatrix} \bar{Q}_{11}^{(k)} & \bar{Q}_{12}^{(k)} & \bar{Q}_{16}^{(k)} & 0 & 0 \\ \bar{Q}_{12}^{(k)} & \bar{Q}_{22}^{(k)} & \bar{Q}_{26}^{(k)} & 0 & 0 \\ \bar{Q}_{16}^{(k)} & \bar{Q}_{26}^{(k)} & \bar{Q}_{66}^{(k)} & 0 & 0 \\ 0 & 0 & 0 & \bar{Q}_{44}^{(k)} & \bar{Q}_{45}^{(k)} \\ 0 & 0 & 0 & \bar{Q}_{45}^{(k)} & \bar{Q}_{55}^{(k)} \end{pmatrix} \begin{pmatrix} \epsilon_x^{(k)} \\ \epsilon_\theta^{(k)} \\ \gamma_{x\theta}^{(k)} \\ \gamma_{\theta z}^{(k)} \\ \gamma_{xz}^{(k)} \end{pmatrix} \tag{3}$$

where $Q_{ij}^{(k)}$ and $\bar{Q}_{ij}^{(k)}$ are given by Viswanathan and Lee (2007).

The strain-displacement relations for conical shells having the radius r is given as

$$\begin{aligned} \epsilon_x &= \frac{\partial u_0}{\partial x} + z \frac{\partial \psi_x}{\partial x}, \quad \epsilon_\theta = \frac{1}{x \sin \alpha} \frac{\partial v_0}{\partial \theta} + \frac{w}{x \sin \alpha} + \frac{z}{x \sin \alpha} \frac{\partial \psi_\theta}{\partial \theta}, \quad \gamma_{xz} = \psi_x + \frac{\partial w}{\partial x}, \\ \gamma_{x\theta} &= \frac{1}{x \sin \alpha} \frac{\partial u_0}{\partial \theta} + \frac{\partial v_0}{\partial x} + z \left(\frac{1}{x \sin \alpha} \frac{\partial \psi_x}{\partial \theta} + \frac{\partial \psi_\theta}{\partial x} \right), \quad \gamma_{\theta z} = \psi_\theta + \frac{1}{x \sin \alpha} \frac{\partial w}{\partial \theta} - \frac{v_0}{x \sin \alpha}, \\ \kappa_x &= \frac{\partial \psi_x}{\partial x}, \quad \kappa_\theta = \frac{1}{x \sin \alpha} \frac{\partial \psi_\theta}{\partial \theta} \quad \text{and} \quad \kappa_{x\theta} = \frac{1}{x \sin \alpha} \frac{\partial \psi_x}{\partial \theta} + \frac{\partial \psi_\theta}{\partial x} \end{aligned} \tag{4}$$

Substituting Eq. (4) into Eq. (3) and then into Eq. (1) we get the equations of stress-resultants and moment resultants as

$$\begin{pmatrix} N_x \\ N_\theta \\ N_{x\theta} \\ M_x \\ M_\theta \\ M_{x\theta} \end{pmatrix} = \begin{pmatrix} A_{11} & A_{12} & A_{16} & B_{11} & B_{12} & B_{16} \\ A_{12} & A_{22} & A_{26} & B_{12} & B_{22} & B_{26} \\ A_{16} & A_{26} & A_{66} & B_{16} & B_{26} & B_{66} \\ B_{11} & B_{12} & B_{16} & D_{11} & D_{12} & D_{16} \\ B_{12} & B_{22} & B_{26} & D_{12} & D_{22} & D_{26} \\ B_{16} & B_{26} & B_{66} & D_{16} & D_{26} & D_{66} \end{pmatrix} \begin{pmatrix} \epsilon_x^0 \\ \epsilon_\theta^0 \\ \gamma_{x\theta}^0 \\ \kappa_x \\ \kappa_\theta \\ \kappa_{x\theta} \end{pmatrix} \tag{5}$$

and

$$\begin{pmatrix} Q_\theta \\ Q_x \end{pmatrix} = K \begin{pmatrix} A_{44} & A_{45} \\ A_{45} & A_{55} \end{pmatrix} \begin{pmatrix} \gamma_{\theta z}^0 \\ \gamma_{xz}^0 \end{pmatrix} \tag{6}$$

The thickness of the k -th layer is assumed in the form

$$h_k(x) = h_{0k} g(x) \tag{7}$$

where h_{0k} is a constant thickness where $g(x) = C_s \sin \pi \left(\frac{x-a}{l} \right)$ and C_s is the coefficients of sinusoidal variation.

Since the thickness is assumed to be varying along the axial direction, we define the elastic coefficients A_{ij} , B_{ij} and D_{ij} (extensional, bending-extensional coupling and bending stiffness's) corresponding to layers of uniform thickness with superscript 'c' as

$$A_{ij} = A_{ij}^c g(x), \quad B_{ij} = B_{ij}^c g(x), \quad D_{ij} = D_{ij}^c g(x)$$

$$A_{ij}^c = \sum_k \bar{Q}_{ij}^{(k)} (z_k - z_{k-1}), \quad B_{ij}^c = \frac{1}{2} \sum_k \bar{Q}_{ij}^{(k)} (z_k^2 - z_{k-1}^2), \tag{8}$$

$$D_{ij}^c = \frac{1}{3} \sum_k \bar{Q}_{ij}^{(k)} (z_k^3 - z_{k-1}^3) \quad \text{for} \quad i, j = 1, 2, 6,$$

and
$$A_{ij}^c = K \sum_k \bar{Q}_{ij}^{(k)} (z_k - z_{k-1}) \quad \text{for} \quad i, j = 4, 5, \tag{9}$$

Here K is the shear correction factor meanwhile z_{k-1} and z_k are boundaries of k -th layer. The value for the shear correction factor K is chosen from the lamination scheme (Madabhusi-Raman and Davalos 1996, Pai and Schulz 1999).

The elastic coefficients A_{16} , A_{26} , A_{45} , B_{11} , B_{12} , B_{22} , B_{66} , D_{16} and D_{26} are identically zero for antisymmetric angle-ply laminates (George 1999, Gibson 1994, Reddy 1997).

The displacement components u_0 , v_0 , w and shear rotations ψ_x , ψ_θ are assumed in a separable form as follows

$$\begin{aligned} u_0(x, \theta, t) &= U(x) e^{n\theta} e^{i\omega t} \\ v_0(x, \theta, t) &= V(x) e^{n\theta} e^{i\omega t} \\ w(x, \theta, t) &= W(x) e^{n\theta} e^{i\omega t} \\ \psi_x(x, \theta, t) &= \Psi_x(x) e^{n\theta} e^{i\omega t} \\ \psi_\theta(x, \theta, t) &= \Psi_\theta(x) e^{n\theta} e^{i\omega t} \end{aligned} \tag{10}$$

where n is the circumferential node number and ω is the angular frequency.

Substituting Eq. (5) and Eq. (6) in to the equilibrium equations and then substituting Eq. (10), the resulting equation becomes as ordinary differential equations in terms of displacements and rotational functions and can be written in the matrix form as

$$\begin{bmatrix} L_{11} & L_{12} & L_{13} & L_{14} & L_{15} \\ L_{21} & L_{22} & L_{23} & L_{24} & L_{25} \\ L_{31} & L_{32} & L_{33} & L_{34} & L_{35} \\ L_{41} & L_{42} & L_{43} & L_{44} & L_{45} \\ L_{51} & L_{52} & L_{53} & L_{54} & L_{55} \end{bmatrix} \begin{Bmatrix} U \\ V \\ W \\ \Psi_x \\ \Psi_\theta \end{Bmatrix} = \begin{Bmatrix} 0 \\ 0 \\ 0 \\ 0 \\ 0 \end{Bmatrix} \quad (11)$$

where

$$\begin{aligned} L_{11} &= A_{11}g \frac{d^2}{dx^2} + A_{11}g' \frac{d}{dx} + A_{11}g \frac{1}{x} \frac{d}{dx} + A_{12}g' \frac{1}{x} - A_{22}g \frac{1}{x^2} + A_{66}g \frac{n^2}{x^2 \sin^2 \alpha} + I_1 \omega^2 \\ L_{12} &= A_{12}g \frac{n}{x \sin \alpha} \frac{d}{dx} + A_{66}g \frac{n}{x \sin \alpha} \frac{d}{dx} + A_{12}g' \frac{n}{x \sin \alpha} - A_{22}g \frac{n}{x^2 \sin \alpha} - A_{66}g \frac{n}{x^2 \sin \alpha} \\ L_{13} &= A_{12}g \frac{1}{x \tan \alpha} \frac{d}{dx} + A_{12}g' \frac{1}{x \tan \alpha} - A_{22}g \frac{1}{x^2 \tan \alpha} \\ L_{14} &= 2B_{16}g \frac{n}{x \sin \alpha} \frac{d}{dx} + B_{16}g' \frac{n}{x \sin \alpha} \\ L_{15} &= B_{16}g \frac{d^2}{dx^2} + B_{16}g' \frac{d}{dx} - B_{26}g \frac{1}{x} \frac{d}{dx} + B_{26}g \frac{1}{x^2} + B_{26}g \frac{n^2}{x^2 \sin^2 \alpha} - B_{16}g' \frac{1}{x} \\ L_{21} &= A_{12}g \frac{n}{x \sin \alpha} \frac{d}{dx} + A_{66}g \frac{n}{x \sin \alpha} \frac{d}{dx} + A_{22}g \frac{n}{x^2 \sin \alpha} + A_{66}g' \frac{n}{x \sin \alpha} + A_{66}g \frac{n}{x^2 \sin \alpha} \\ L_{22} &= A_{66}g \frac{d^2}{dx^2} + A_{66}g' \frac{d}{dx} + A_{66}g \frac{1}{x} \frac{d}{dx} + A_{22}g \frac{n^2}{x^2 \sin^2 \alpha} - kA_{44}g \frac{1}{x^2 \tan^2 \alpha} - A_{66}g' \frac{1}{x} - A_{66}g \frac{1}{x^2} + I_1 \omega^2 \\ L_{23} &= A_{22}g \frac{n}{x^2 \sin \alpha \tan \alpha} + KA_{44}g \frac{n}{x^2 \sin \alpha \tan \alpha} \\ L_{24} &= B_{16}g \frac{d^2}{dx^2} + B_{16}g' \frac{d}{dx} + 2B_{16}g \frac{1}{x} \frac{d}{dx} + B_{26}g \frac{1}{x} \frac{d}{dx} + B_{26}g' \frac{1}{x} + B_{26}g \frac{1}{x^2} + B_{26}g \frac{n^2}{x^2 \sin^2 \alpha} \\ L_{25} &= 2B_{26}g \frac{n}{x \sin \alpha} \frac{d}{dx} + KA_{44}g \frac{1}{x \tan \alpha} + B_{26}g' \frac{n}{x \sin \alpha} \\ L_{31} &= -A_{12}g \frac{1}{x \tan \alpha} \frac{d}{dx} - A_{22}g \frac{1}{x^2 \tan \alpha} \\ L_{32} &= -A_{22}g \frac{n}{x^2 \sin \alpha \tan \alpha} - KA_{44}g \frac{n}{x^2 \sin \alpha \tan \alpha} \\ L_{33} &= KA_{55}g \frac{d^2}{dx^2} + KA_{55}g' \frac{d}{dx} + KA_{55}g \frac{1}{x} \frac{d}{dx} - A_{22}g \frac{1}{x^2 \tan^2 \alpha} + KA_{44}g \frac{n^2}{x^2 \sin^2 \alpha} + I_1 \omega^2 \\ L_{34} &= KA_{55}g \frac{d}{dx} - B_{26}g \frac{n}{x^2 \sin \alpha \tan \alpha} + KA_{55}g' + KA_{55}g \frac{1}{x} \end{aligned}$$

$$\begin{aligned}
 L_{35} &= -B_{26}g \frac{1}{x \tan \alpha} \frac{d}{dx} + KA_{44}g \frac{n}{x \sin \alpha} + B_{26}g \frac{1}{x^2 \tan \alpha} \\
 L_{41} &= 2B_{16}g \frac{n}{x \sin \alpha} \frac{d}{dx} + B_{16}g \frac{n}{x \sin \alpha} \\
 L_{42} &= B_{16}g \frac{d^2}{dx^2} - B_{26}g \frac{1}{x} \frac{d}{dx} + B_{16}g \frac{d}{dx} - B_{16}g \frac{1}{x} + B_{26}g \frac{1}{x^2} + B_{26}g \frac{n^2}{x^2 \sin^2 \alpha} \\
 L_{43} &= -KA_{55}g \frac{d}{dx} + B_{26}g \frac{n}{x^2 \sin \alpha \tan \alpha} \\
 L_{44} &= D_{11}g \frac{d^2}{dx^2} + D_{11}g \frac{d}{dx} + D_{11}g \frac{1}{x} \frac{d}{dx} + D_{12}g \frac{1}{x} - D_{22}g \frac{1}{x^2} + D_{66}g \frac{n^2}{x^2 \sin^2 \alpha} - KA_{55}g + I_3 \omega^2 \\
 L_{45} &= D_{12}g \frac{n}{x \sin \alpha} \frac{d}{dx} + D_{66}g \frac{n}{x \sin \alpha} \frac{d}{dx} + D_{12}g \frac{n}{x \sin \alpha} - D_{22}g \frac{n}{x^2 \sin \alpha} - D_{66}g \frac{n}{x^2 \sin \alpha} \\
 L_{51} &= B_{16}g \frac{d^2}{dx^2} + B_{16}g \frac{d}{dx} + 2B_{16}g \frac{1}{x} \frac{d}{dx} + B_{26}g \frac{1}{x} \frac{d}{dx} + B_{26}g \frac{1}{x} + B_{26}g \frac{1}{x^2} + B_{26}g \frac{n^2}{x^2 \sin^2 \alpha} \\
 L_{52} &= KA_{44}g \frac{1}{x \tan \alpha} + B_{26}g \frac{n}{x \sin \alpha} + 2B_{26}g \frac{n}{x \sin \alpha} \frac{d}{dx} \\
 L_{53} &= B_{26}g \frac{1}{x \tan \alpha} \frac{d}{dx} - KA_{44}g \frac{n}{x \sin \alpha} + B_{26}g \frac{1}{x \tan \alpha} + B_{26}g \frac{1}{x^2 \tan \alpha} \\
 L_{54} &= D_{66}g \frac{n}{x \sin \alpha} \frac{d}{dx} + D_{12}g \frac{n}{x \sin \alpha} \frac{d}{dx} + D_{66}g \frac{n}{x \sin \alpha} + D_{66}g \frac{n}{x^2 \sin \alpha} + D_{22}g \frac{n}{x^2 \sin \alpha} \\
 L_{55} &= D_{66}g \frac{d^2}{dx^2} + D_{66}g \frac{1}{x} \frac{d}{dx} + D_{66}g \frac{d}{dx} - KA_{44}g - D_{66}g \frac{1}{x} - D_{66}g \frac{1}{x^2} + D_{22}g \frac{n^2}{x^2 \sin^2 \alpha} + I_3 \omega^2
 \end{aligned}$$

The following non-dimensional parameters are introduced:

$$X = \frac{x-a}{l}, \quad a \leq x \leq b \quad \text{and} \quad X \in [0,1]$$

$$\lambda = \omega \ell \sqrt{\frac{I_1}{A_{11}}}, \quad \text{a frequency parameter}$$

$$\gamma = \frac{h_0}{r_a}, \quad \gamma' = \frac{h_0}{a}, \quad \text{ratios of thickness to radius and to a length}$$

$$\beta = \frac{a}{b}, \quad \text{a length ratio}$$

$$\delta_k = \frac{h_k}{h}, \quad \text{relative layer thickness of the } k \text{-th layer.}$$

$$G(X) = C_s \sin(\pi X), \quad \text{thickness variation.} \tag{12}$$

The new set of differential equations are obtained as

$$\begin{bmatrix} L_{11}^* & L_{12}^* & L_{13}^* & L_{14}^* & L_{15}^* \\ L_{21}^* & L_{22}^* & L_{23}^* & L_{24}^* & L_{25}^* \\ L_{31}^* & L_{32}^* & L_{33}^* & L_{34}^* & L_{35}^* \\ L_{41}^* & L_{42}^* & L_{43}^* & L_{44}^* & L_{45}^* \\ L_{51}^* & L_{52}^* & L_{53}^* & L_{54}^* & L_{55}^* \end{bmatrix} \begin{Bmatrix} \bar{U} \\ \bar{V} \\ \bar{W} \\ \bar{\Psi}_X \\ \bar{\Psi}_\Theta \end{Bmatrix} = \begin{Bmatrix} 0 \\ 0 \\ 0 \\ 0 \\ 0 \end{Bmatrix} \tag{13}$$

where

$$\begin{aligned} L_{11}^* &= \frac{d^2}{dX^2} + \left(\frac{G'}{G} + p \right) \frac{d}{dX} + s_2 \frac{G'}{G} p - s_3 p^2 + s_{10} n^2 p^2 \operatorname{cosec}^2 \alpha + \lambda^2 \\ L_{12}^* &= (s_2 + s_{10}) np \operatorname{cosec} \alpha \frac{d}{dX} + \left(s_2 \frac{G'}{G} - s_3 p - s_{10} p \right) np \operatorname{cosec} \alpha \\ L_{13}^* &= s_2 p \cot \alpha \frac{d}{dX} + \left(s_2 \frac{G'}{G} - s_3 p \right) p \cot \alpha \\ L_{14}^* &= 2s_{15} np \operatorname{cosec} \alpha \frac{d}{dX} + s_{15} \frac{G'}{G} np \operatorname{cosec} \alpha \\ L_{15}^* &= s_{15} \frac{d^2}{dX^2} + \left(s_{15} \frac{G'}{G} - s_{16} p \right) \frac{d}{dX} + \left(s_{16} p + s_{16} n^2 p \operatorname{cosec}^2 \alpha - s_{15} \frac{G'}{G} \right) p \\ L_{21}^* &= (s_2 + s_{10}) np \operatorname{cosec} \alpha \frac{d}{dX} + \left(s_{10} \frac{G'}{G} + s_{10} p + s_3 p \right) np \operatorname{cosec} \alpha \\ L_{22}^* &= s_{10} \frac{d^2}{dX^2} + s_{10} \left(\frac{G'}{G} + p \right) \frac{d}{dX} + \left(-s_{10} \frac{G'}{G} - s_{10} p - Ks_{13} p \cot^2 \alpha + s_3 p n^2 \operatorname{cosec}^2 \alpha \right) p + \lambda^2 \\ L_{23}^* &= (s_3 + Ks_{13}) p^2 n \operatorname{cosec} \alpha \cot \alpha \\ L_{24}^* &= s_{15} \frac{d^2}{dX^2} + \left(s_{15} \frac{G'}{G} + s_{16} p + 2s_{15} p \right) \frac{d}{dX} + s_{16} \left(\frac{G'}{G} + p + p n^2 \operatorname{cosec}^2 \alpha \right) p \\ L_{25}^* &= 2s_{16} p n \operatorname{cosec} \alpha \frac{d}{dX} + \left(Ks_{13} \cot \alpha + s_{16} \frac{G'}{G} n \operatorname{cosec} \alpha \right) p \\ L_{31}^* &= -s_2 p \cot \alpha \frac{d}{dX} - s_3 p^2 \cot \alpha \\ L_{32}^* &= (-s_3 - Ks_{13}) p^2 n \operatorname{cosec} \alpha \cot \alpha \\ L_{33}^* &= Ks_{14} \frac{d^2}{dX^2} + Ks_{14} \left(\frac{G'}{G} + p \right) \frac{d}{dX} + \left(-s_3 \cot^2 \alpha + Ks_{13} n^2 \operatorname{cosec}^2 \alpha \right) p^2 + \lambda^2 \end{aligned}$$

$$\begin{aligned}
 L_{34}^* &= Ks_{14} \frac{d}{dX} - s_{16}p^2n \operatorname{cosec} \alpha \cot \alpha + Ks_{14} \frac{G'}{G} + Ks_{14}p \\
 L_{35}^* &= -s_{16}p \cot \alpha \frac{d}{dX} + (Ks_{13}n \operatorname{cosec} \alpha + s_{16}p \cot \alpha) p \\
 L_{41}^* &= 2s_{15}np \operatorname{cosec} \alpha \frac{d}{dX} + s_{15} \frac{G'}{G} np \operatorname{cosec} \alpha \\
 L_{42}^* &= s_{15} \frac{d^2}{dX^2} + \left(s_{15} \frac{G'}{G} - s_{16}p \right) \frac{d}{dX} + \left(-s_{15} \frac{G'}{G} + s_{16}p + s_{16}pn^2 \operatorname{cosec}^2 \alpha \right) p \\
 L_{43}^* &= -Ks_{14} \frac{d}{dX} + s_{16}p^2n \operatorname{cosec} \alpha \cot \alpha \\
 L_{44}^* &= s_7 \frac{d^2}{dX^2} + s_7 \left(\frac{G'}{G} + p \right) \frac{d}{dX} + \left(s_8 \frac{G'}{G} p - s_9p^2 + s_{12}p^2n^2 \operatorname{cosec}^2 \alpha - Ks_{14} \right) + \lambda^2 p_1 \\
 L_{45}^* &= (s_8n \operatorname{cosec} \alpha + s_{12}n \operatorname{cosec} \alpha) p \frac{d}{dX} + \left(s_8 \frac{G'}{G} - s_9p - s_{12}p \right) pn \operatorname{cosec} \alpha \\
 L_{51}^* &= s_{15} \frac{d^2}{dX^2} + \left(s_{15} \frac{G'}{G} + 2s_{15}p + s_{16}p \right) \frac{d}{dX} + s_{16} \left(\frac{G'}{G} + p + pn^2 \operatorname{cosec}^2 \alpha \right) p \\
 L_{52}^* &= 2s_{16}pn \operatorname{cosec} \alpha \frac{d}{dX} + \left(s_{16} \frac{G'}{G} n \operatorname{cosec} \alpha + Ks_{13} \cot \alpha \right) p \\
 L_{53}^* &= s_{16}p \cot \alpha \frac{d}{dX} + \left(s_{16} \frac{G'}{G} \cot \alpha - Ks_{13}n \operatorname{cosec} \alpha + s_{16}p \cot \alpha \right) p \\
 L_{54}^* &= (s_{12} + s_8) pn \operatorname{cosec} \alpha \frac{d}{dX} + \left(s_{12} \frac{G'}{G} + s_{12}p + s_9p \right) pn \operatorname{cosec} \alpha \\
 L_{55}^* &= s_{12} \frac{d^2}{dX^2} + s_{12} \left(\frac{G'}{G} + p \right) \frac{d}{dX} - \left(s_{12} \frac{G'}{G} p + s_{12}p^2 - s_9p^2n^2 \operatorname{cosec}^2 \alpha + Ks_{13} \right) + \lambda^2 p_1
 \end{aligned}$$

2.1 Spline collocation procedure

The displacement functions U, V, W and rotational functions Ψ_x, Ψ_θ are approximated by cubic spline functions in the range of $X \in [0, 1]$ as

$$\begin{aligned}
 \bar{U}(X) &= \sum_{i=0}^2 a_i X^i + \sum_{j=0}^{N-1} b_j (X - X_j)^3 H(X - X_j) \\
 \bar{V}(X) &= \sum_{i=0}^2 c_i X^i + \sum_{j=0}^{N-1} d_j (X - X_j)^3 H(X - X_j)
 \end{aligned}$$

$$\begin{aligned}
\bar{W}(X) &= \sum_{i=0}^2 e_i X^i + \sum_{j=0}^{N-1} f_j (X - X_j)^3 H(X - X_j) \\
\bar{\Psi}_X(X) &= \sum_{i=0}^2 g_i X^i + \sum_{j=0}^{N-1} p_j (X - X_j)^3 H(X - X_j) \\
\bar{\Psi}_\theta(X) &= \sum_{i=0}^2 l_i X^i + \sum_{j=0}^{N-1} q_j (X - X_j)^3 H(X - X_j)
\end{aligned} \tag{14}$$

Here, $H(X-X_j)$ is the Heaviside step functions. The range of X is divided in to N subintervals, at the points $X=X_s$, $s=1,2,3,\dots,N-1$. The width of each subinterval is $1/N$ and $X_s=s/N$ ($s=0,1,2,\dots,N$), since the knots X_s are chosen equally spaced.

The assumed spline functions given in Eq. (14) are approximated at the nodes (coincide with the knots) and these splines satisfy the differential equations given in Eq. (13), at all X_s and resulting into the homogeneous system of $(5N+5)$ equations in the $(5N+15)$ unknown spline coefficients.

The boundary conditions considered are as follows.

(i) Clamped–Clamped (C–C). Both ends are clamped.

$$U = V = W = \Psi_X = \Psi_\theta = 0 \text{ at } X = 0 \text{ and } X = 1$$

(ii) Simply supported (S–S). Both ends are simply-supported.

$$V = W = N_X = M_X = \Psi_\theta = 0 \text{ at } X = 0 \text{ and } X = 1$$

(iii) Clamped–Free (C–F). (Small end is clamped and the large end is simply supported)

$$U = V = W = \Psi_X = \Psi_\theta = 0 \text{ at } X = 0 \text{ and } N_X = M_X = Q_X = N_{X\theta} = M_{X\theta} = 0 \text{ at } X = 1$$

By applying any one of the boundary conditions, one can obtain 10 more equations on spline coefficients. Combining these 10 equations with the earlier $(5N+5)$ equations, we get $(5N+15)$ homogeneous equations in the same number unknowns. Thus, we have a generalized eigenvalue problem in the form

$$[M]\{q\} = \lambda^2[P]\{q\} \tag{15}$$

where $[M]$ and $[P]$ are the square matrices, $\{q\}$ is the column matrix of the spline coefficients and λ is the eigenfrequency parameter.

3. Numerical results and discussion

The present formulation is applied to investigate the free vibration of anti-symmetric angle-ply conical shells having sinusoidal thickness variation under three different support conditions. All numerical computations in this section, unless otherwise stated, three materials are considered: Kevlar-49/epoxy (KE), Graphite/Epoxy (AS4/3501-6) (GE) and E-glass epoxy (EGE). Two and four layered shells having ply orientations $30^\circ/-30^\circ$, $45^\circ/-45^\circ$, $30^\circ/-45^\circ/45^\circ/-30^\circ$, $30^\circ/-60^\circ/60^\circ/-30^\circ$, $60^\circ/-45^\circ/45^\circ/-60^\circ$ and three support conditions C-C, S-S and C-F are considered.

3.1 Convergence study

In this subsection the frequency parameter with respect to different configurations are carried out to confirm the convergence of the cubic spline method for anti-symmetric angle-ply conical shells having variable thickness. The number of subintervals N of the range $X \in [0,1]$. The value of N started from 4 and finally it is fixed for $N=16$, since for the next value of N , the percent changes in the values of λ are very low, the maximum being 3%.

3.2 Validation

The comparative study have been made for constant thickness of the conical shells and given in Viswanathan *et al.* (2015). The results are the reduced case of the present study to a constant thickness of the shells.

3.3 Effect of different parameters of the conical shell and support conditions

Tables 1-3 shows the effect of sinusoidal thickness variation on fundamental frequency parameter for C-C, S-S and C-F support conditions respectively. Table 1 shows that ply-angle $30^\circ/-45^\circ/45^\circ/-30^\circ$ shows the highest frequency parameter value and $45^\circ/-45^\circ$ shows lowest. For Table 2 ply-angle $45^\circ/-45^\circ$ depicts the highest frequency parameter and $30^\circ/-30^\circ$ depicts lowest. In Table 3 contrary to Table 1 ply-angle $45^\circ/-45^\circ$ shows the highest and $30^\circ/-45^\circ/45^\circ/-30^\circ$ shows

Table 1 Influence of sinusoidal thickness variation C_s on the fundamental frequency parameter λ under C-C support condition. $n=2, \gamma=0.05, \alpha=60^\circ$ and $\beta=0.5$

C_s	$30^\circ/-30^\circ$	$45^\circ/-45^\circ$	$30^\circ/-45^\circ/45^\circ/-30^\circ$	$30^\circ/-60^\circ/60^\circ/-30^\circ$
	(KE/KE)	(KE/KE)	(KE/EGE/EGE/KE)	(KE/EGE/EGE/KE)
	λ	λ	λ	λ
-0.5	1.89811	1.69789	1.978668	1.80633
-0.3	1.90091	1.66187	1.988876	1.84567
-0.1	1.85594	1.65801	1.989119	1.87303
0.1	1.87737	1.61623	1.985853	1.89316
0.3	1.87101	1.65929	1.981819	1.84567
0.5	1.89773	1.68451	1.977488	1.80719

Table 2 Influence of sinusoidal thickness variation C_s on the fundamental frequency parameter λ under S-S support condition. $n=2, \gamma=0.05, \alpha=60^\circ$ and $\beta=0.5$

C_s	$30^\circ/-30^\circ$	$45^\circ/-45^\circ$	$30^\circ/-45^\circ/45^\circ/-30^\circ$	$30^\circ/-60^\circ/60^\circ/-30^\circ$
	(KE/KE)	(KE/KE)	(KE/EGE/EGE/KE)	(KE/EGE/EGE/KE)
	λ	λ	λ	λ
-0.5	0.464538	0.846208	0.658875	0.768956
-0.3	0.448166	0.830173	0.673435	0.754662
-0.1	0.441287	0.822360	0.679602	0.747286
0.1	0.439051	0.817331	0.682040	0.745142
0.3	0.439343	0.813349	0.682908	0.748210
0.5	0.441047	0.834038	0.683260	0.755064

Table 3 Influence of sinusoidal thickness variation C_s on the fundamental frequency parameter λ under C-F support condition. $n=2$, $\gamma=0.05$, $\alpha=60^\circ$ and $\beta=0.5$

C_s	$30^\circ/-30^\circ$	$45^\circ/-45^\circ$	$30^\circ/-45^\circ/45^\circ/-30^\circ$	$30^\circ/-60^\circ/60^\circ/-30^\circ$
	(KE/KE)	(KE/KE)	(KE/EGE/EGE/KE)	(KE/EGE/EGE/KE)
	λ	λ	λ	λ
-0.5	0.459758	0.669860	0.216367	0.483233
-0.3	0.462389	0.676056	0.215041	0.467554
-0.1	0.456876	0.678195	0.228210	0.452433
0.1	0.448064	0.669158	0.235597	0.453609
0.3	0.437928	0.657365	0.208621	0.460534
0.5	0.427357	0.664105	0.216380	0.483723

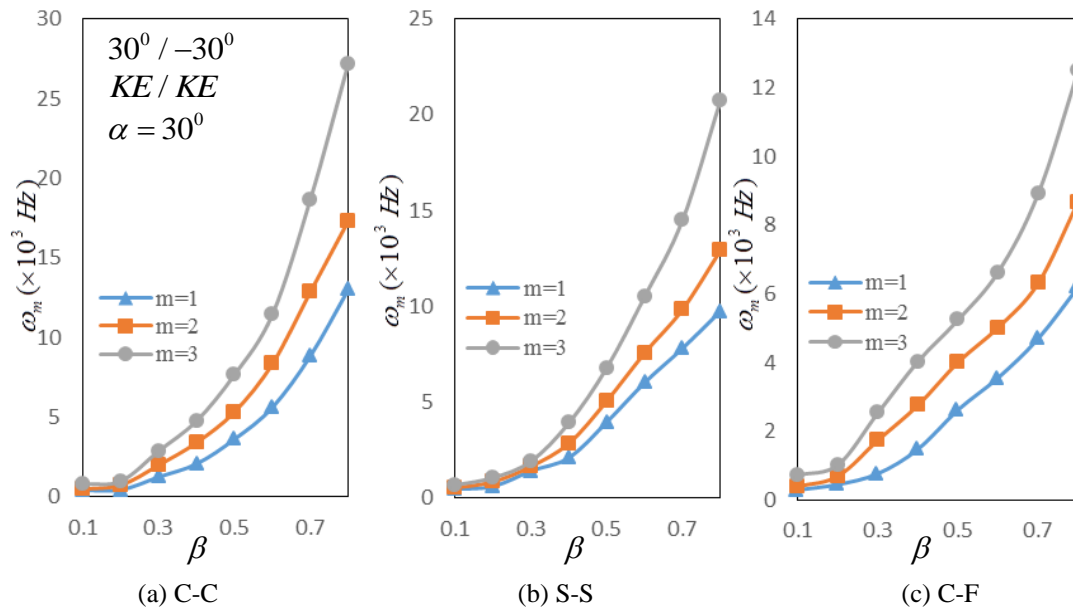


Fig. 2 The angular frequency discrepancies with respect to aspect ratio for two layered shells: $C_s=0.25$, $n=2$ and $\gamma=0.05$

the lowest frequency parameter value. It is evident from three tables that fundamental frequency parameter differs with the increase of sinusoidal thickness variation. In addition to that fundamental frequency discrepancies shows that the values of fundamental frequency is highest for C-C followed by S-S and C-F support conditions. Except for $30^\circ/-30^\circ$ ply-angle for which the frequency value is almost same for S-S and C-F support condition.

Figs. 2 (a)-(c) enables us to examine the effect of aspect ratio which is actually length ratio of the conical shell on angular frequency behavior. The lamination angle $30^\circ/-30^\circ$, material KE/KE, cone angle $\alpha=30^\circ$, coefficient of sinusoidal variation $C_s=0.25$, circumferential node number $n=2$ and ratios of thickness to radius $\gamma=0.05$ are fixed. The general behavior of three angular frequency curves is similar to each other, in which the angular frequency value ω_m ($m=1,2,3$) remains almost same between $0.1 < \beta < 0.2$ and increases afterwards between $0.3 < \beta < 0.8$. For conical shell with C-C

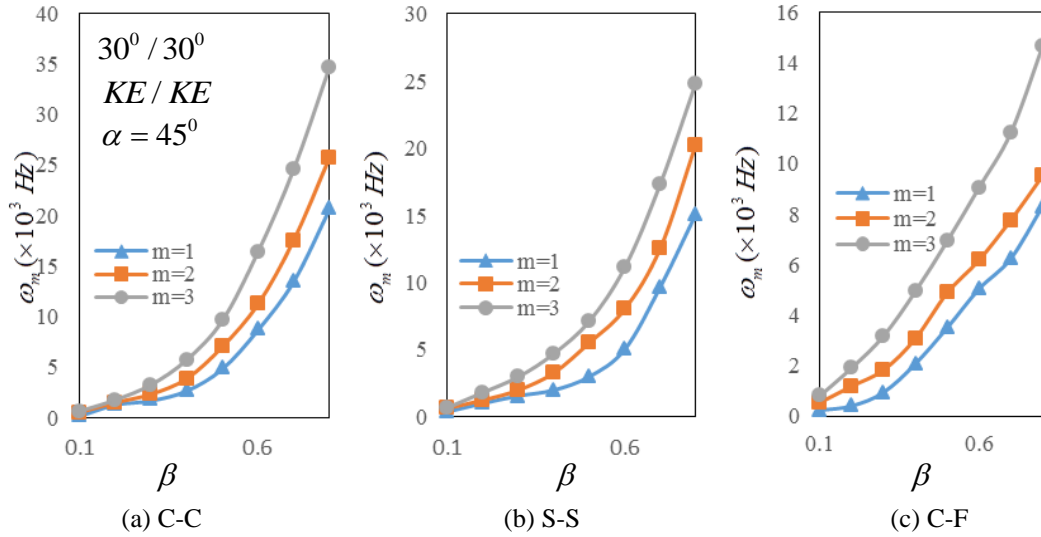


Fig. 3 The angular frequency discrepancies with respect to aspect ratio for two layered shells: $C_s=0.25$, $n=2$ and $\gamma=0.05$

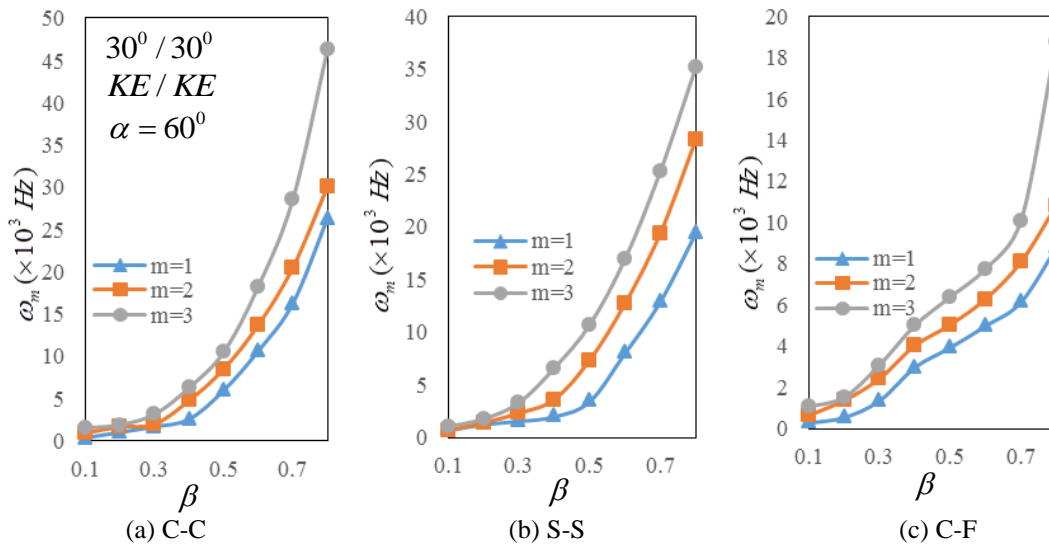


Fig. 4 The angular frequency discrepancies with respect to aspect ratio for two layered shells: $C_s=0.25$, $n=2$ and $\gamma=0.05$

and S-S support conditions the trend of the curves are identical as compare to the curve of C-F support condition. Examining the angular frequency discrepancies of three support conditions shows that the value of the angular frequency is highest for C-C support conditions followed by S-S and C-F.

Effect of different cone angles on the relationship between aspect ratio and angular frequency is presented in Figs. 3 and 4. The characteristic curve are similar as for Fig. 2. Finally concluded that

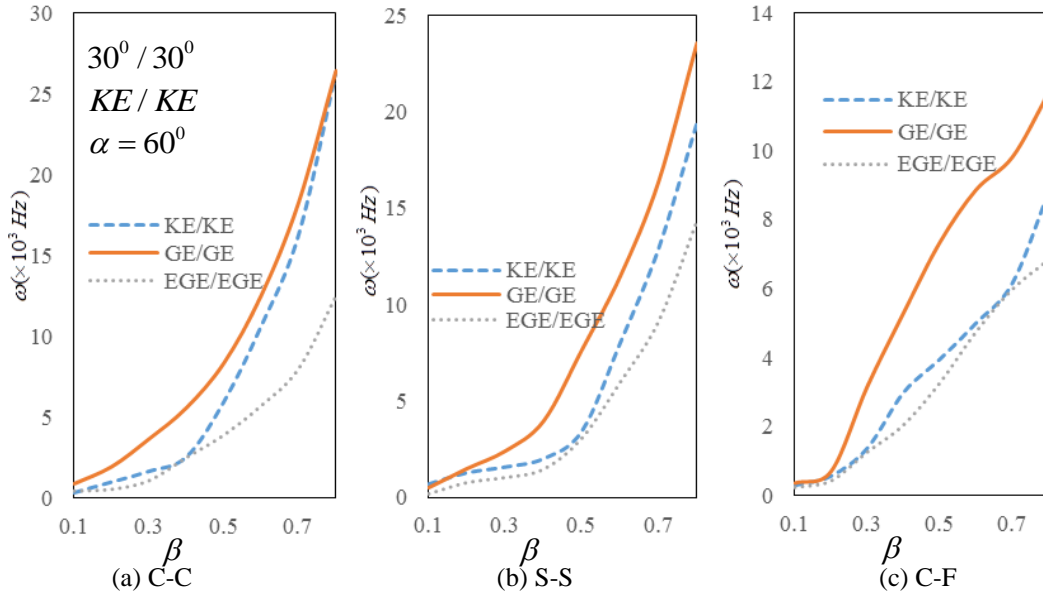


Fig. 5 The influence of aspect ratio on the fundamental angular frequency of two layered shells having different lamination materials: $C_s=0.25$, $n=2$ and $\gamma=0.05$

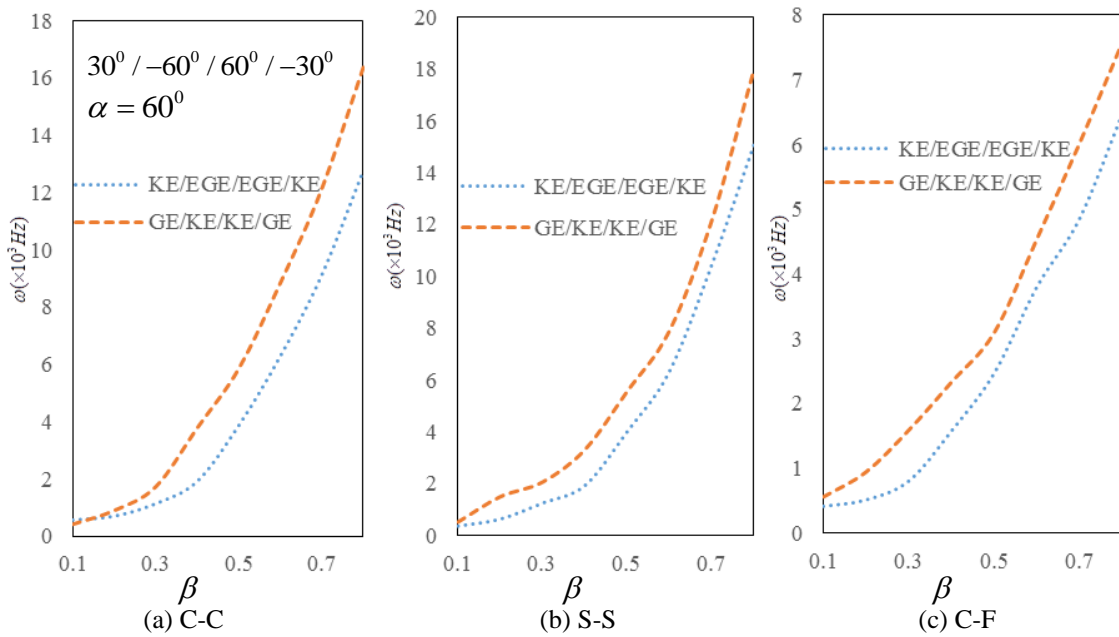


Fig. 6 The influence of aspect ratio on the fundamental angular frequency of four layered shells having different lamination materials: $C_s=0.25$, $n=2$ and $\gamma=0.05$

the angular frequency value varies for different cone angles with the increase of aspect ratio.

Fig. 5 demonstrates the different lamination materials effecting the fundamental angular

frequency with the increase of aspect ratio of two layered shell for different support conditions. Figs. 5 (a)-(c) exhibits that the value of angular frequency for lamination material $GE > KE > EGE$ for all the support conditions considered. The curvature of the curves for C-F support conditions is slightly different with that of C-C and S-S support conditions.

Two different combination of layer materials are considered in Figs. 6(a)-(c). Generally the angular frequency increases as the aspect ratio increases. The increase is slow between $0.1 < \beta < 0.3$ and strict afterwards. Moreover, lamination combination $KE/EGE/EGE/KE$ intends lower frequency than $GE/KE/KE/GE$ under three support conditions considered.

Four layered shells with lamination and material scheme as $30^\circ/-45^\circ/45^\circ/-30^\circ$ ($GE/KE/KE/GE$) are considered to study the effect of cone angle on the frequency parameter value in Figs. 7(a)-(c). Characteristics curve shows nearly similar pattern for three figures showing strict decrease in the value of frequency parameter between $10^\circ < \alpha < 30^\circ$ and becomes slow afterwards.

Different lamination angle $30^\circ/-60^\circ/60^\circ/-30^\circ$ ($GE/KE/KE/GE$) is considered in Fig. 8 as compare to Fig. 7. The frequency parameter values for C-C support condition is lowest as compare to other two. The curvature of the curve is similar as in Fig. 7. Moreover for S-S support conditions the difference between the values of first and second mode is more than other boundary condition.

The influence of cone angle on the variation of frequency parameter value is studied four layered shells in Fig. 9 under C-C support conditions. The frequency value decreases until $\alpha=30^\circ$ and becomes almost linear afterwards. Examining the effect of circumferential node number $n=2$ and $n=4$ it is concluded the value of the frequency parameter lowers with the increase of circumferential node number.

Fig. 10 (a) and (b) intends to study the effect of different lamination material scheme and cone angle on frequency parameter value for C-C support conditions. The general behavior of three

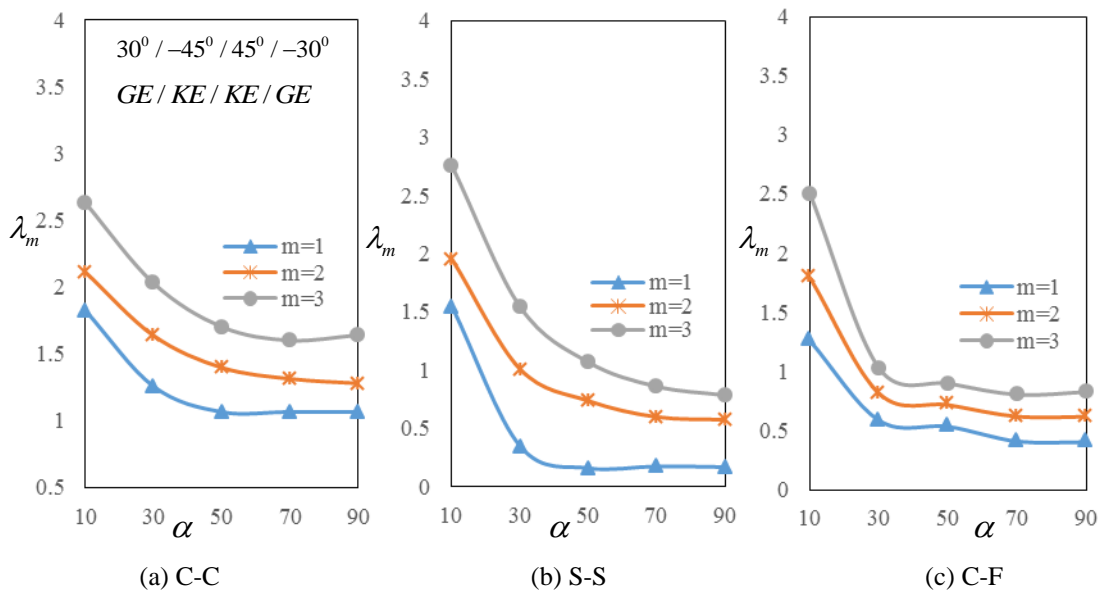


Fig. 7 The frequency parameter discrepancies with respect to cone angle for four layered shells: $C_s=0.25$, $n=2$, $\gamma'=0.5$ and $\beta=0.5$

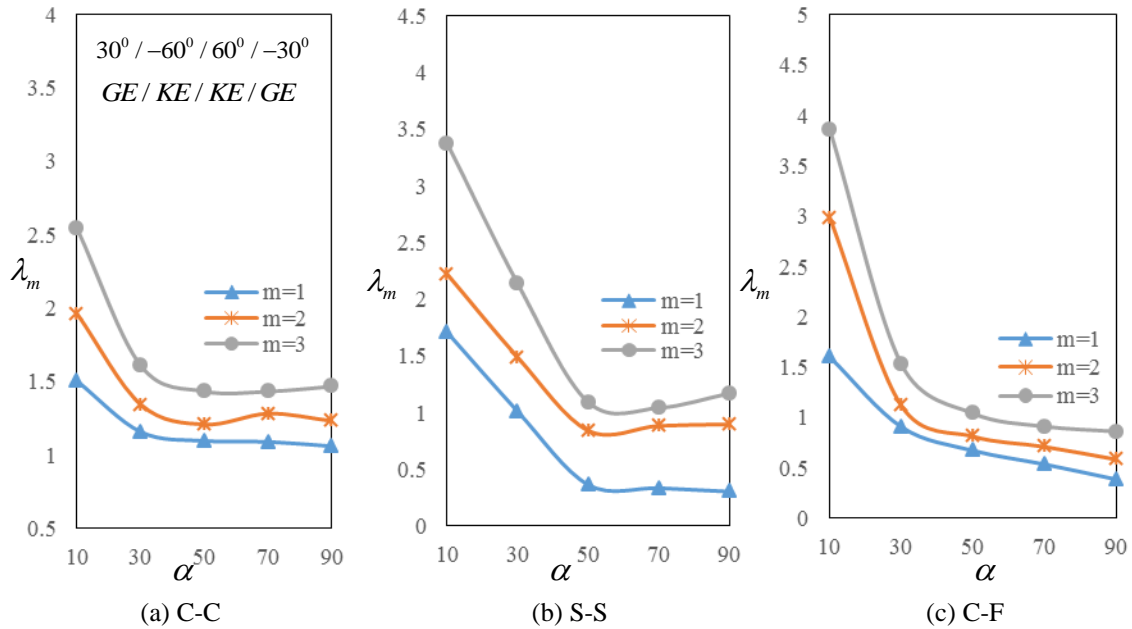


Fig. 8 The frequency parameter discrepancies with respect to cone angle for four layered shells: $C_s=0.25$, $n=2$, $\gamma'=0.5$ and $\beta=0.5$

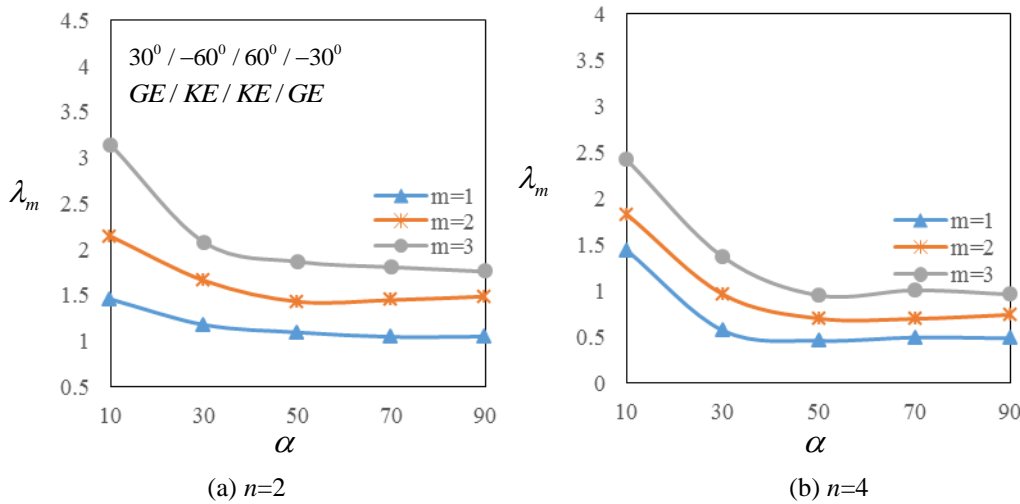


Fig. 9 The frequency parameter discrepancies with respect to cone angle for four layered shells under C-C boundary conditions: $C_s=0.5$, $\gamma'=0.5$ and $\beta=0.5$

modes is similar. Specifically, curvature of the modes $m=2,3$ is steeper than that of $m=1$ for both figures. Moreover, it is concluded that shell consisting of KE/EGE/EGE/KE shows higher frequency as compare to EGE/GE/GE/EGE material.

Four layered shells consisting of different lamination materials are studied in Fig. 11 under C-C

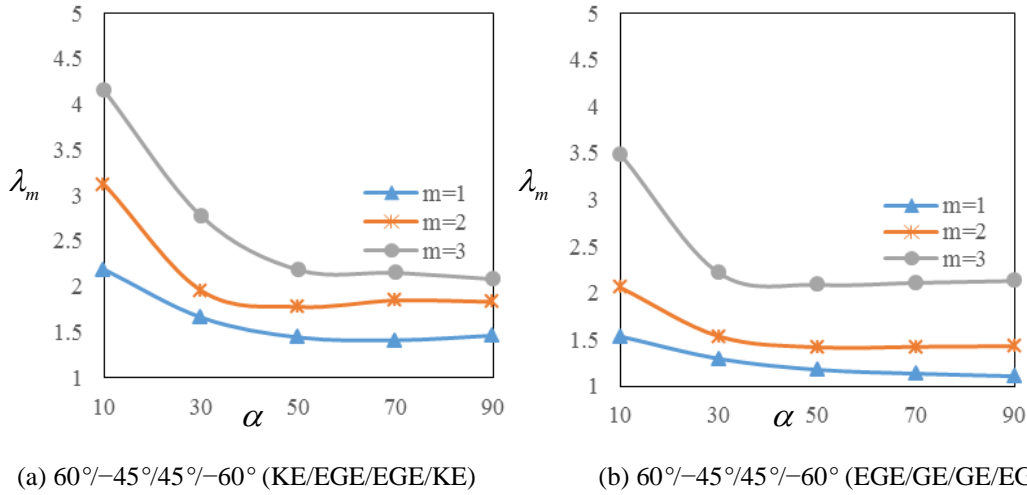


Fig. 10 The frequency parameter discrepancies with respect to cone angle for four layered shells under C-C boundary conditions: $n=2$, $C_s=0.25$, $\gamma'=0.5$ and $\beta=0.5$

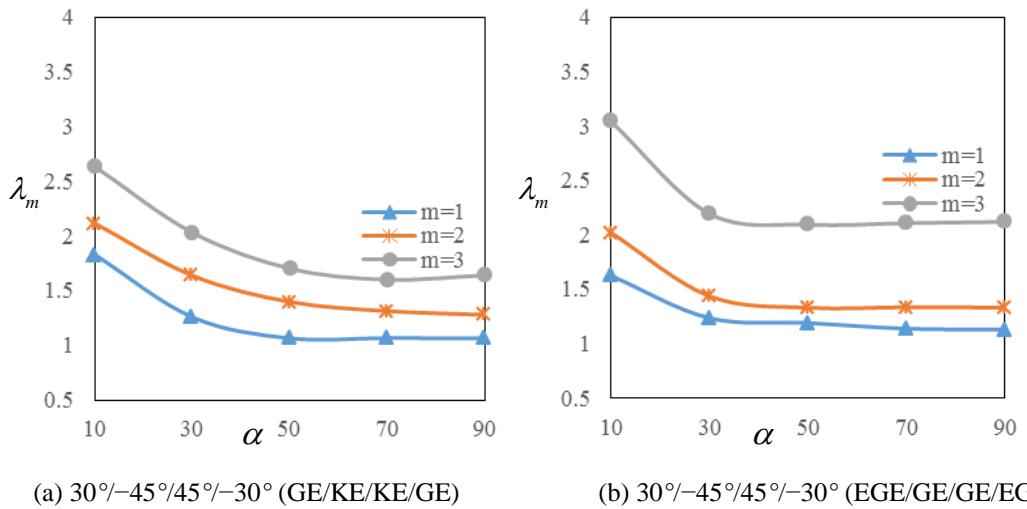


Fig. 11 The frequency parameter discrepancies with respect to cone angle for four layered shells under C-C boundary conditions: $n=2$, $C_s=0.25$, $\gamma'=0.5$ and $\beta=0.5$

support conditions. It is seen that with the increase of cone angle the frequency parameter value decreases strictly until $\alpha=30^\circ$ and the decrease is slow afterwards. Moreover, the difference in the frequency value of mode $m=2,3$ is less for GE/KE/KE/GE than EGE/GE/GE/EGE material shell.

Fig. 12 presents the impact of cone angle on the frequency parameter for two layered shells comprise of different materials KE and GE under S-S support conditions. General trend of the curvature for three modes is similar but the effects of using different materials alter the frequency which may be beneficial for designers to design required structure.

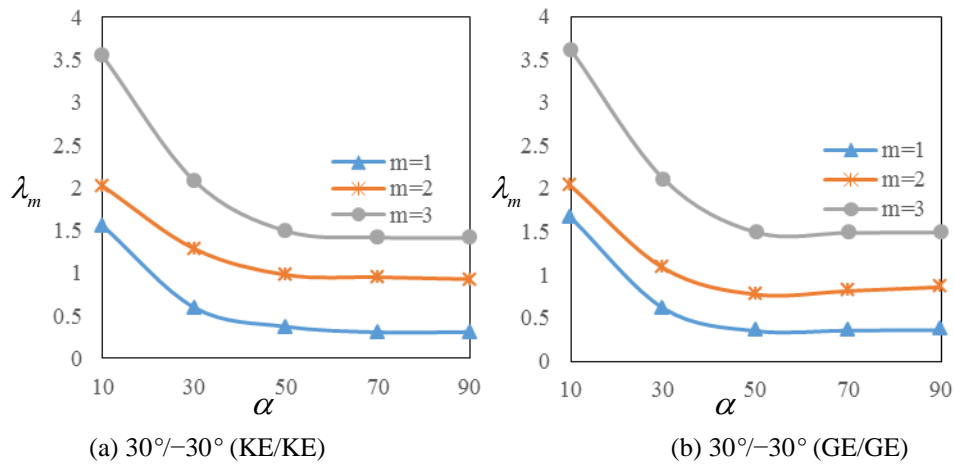


Fig. 12 The frequency parameter discrepancies with respect to cone angle for four layered shells under S-S boundary conditions: $n=2$, $C_s=0.25$, $\gamma'=0.5$ and $\beta=0.5$

4. Conclusions

The present study investigates the free vibration of anti-symmetric angle-ply conical shells having sinusoidal thickness variation under shear deformation theory. The vibrational behavior of conical shells is analyzed for three different support conditions. The vibration characteristic of the shells is examined for cone angle, aspect ratio, sinusoidal thickness variation, layer number and stacking sequence. It is concluded that variation of the geometric parameters and materials affect the frequency, whether this effect is significant or marginal may be valuable for the engineers of related field.

Acknowledgments

This work was supported by GUP Project Vote No. 11H90, under Research Management Centre (RMC), Universiti Teknologi Malaysia, Johor Bahru, Johor, Malaysia and Dr. Saira Javed thanks to Research Management Centre (RMC), Universiti Teknologi Malaysia for her Post-doctoral Fellowship scheme under the Vote No. 02E17.

References

- Akbari, M., Kiani, Y., Aghdam, M.M. and Eslami, M.R. (2014), "Free vibration of FGM Lévy conical panels", *Compos. Struct.*, **116**, 732-746.
- Alibeigloo, A. (2009), "Static and vibration analysis of axi-symmetric angle-ply laminated cylindrical shell using state space differential quadrature method", *Int. J. Press. Ves. Pip.*, **86**, 738-747.
- Ansari, R., Faghhi Shojaei, M., Rouhi, H. and Hosseinzadeh, M. (2015), "A novel variational numerical method for analyzing the free vibration of composite conical shells", *Appl. Math. Model.*, **39**(10), 2849-2860.

- Chernobryvko, M.V., Avramov, K.V., Romanenko, V.N., Batutina, T.J. and Tonkonogenko, A.M. (2014), "Free linear vibrations of thin axisymmetric parabolic shells", *Meccanica*, **49**(12), 2839-2845.
- Dey, S. and Karmakar, A. (2012), "Natural frequencies of delaminated composite rotating conical shells-A finite element approach", *Finite Elem. Anal. Des.*, **56**, 41-51.
- Firouz-Abadi, R.D., Rahmanian, M. and Amabili, M. (2014), "Free vibration of moderately thick conical shells using a higher order shear deformable theory", *J. Vib. Acoust.*, **136**(5), 051001.
- George, H.S. (1999), *Laminar Composites*, Butterworth-Heinemann publications, USA.
- Gibson, R.F. (1994), *Principles of Composite Material Mechanics*, McGraw-Hill, Singapore.
- Jin, G., Ma, X., Shi, S., Ye, T. and Liu, Z. (2014), "A modified Fourier series solution for vibration analysis of truncated conical shells with general boundary conditions", *Appl. Acoust.*, **85**, 82-96.
- Khare, R.K., Kant, T. and Garg, A.K. (2004), "Free vibration of composite and sandwich laminates with a higher-order facet shell element", *Compos. Struct.*, **65**(3-4), 405-418.
- Kang, J.H. (2014), "Vibration analysis of complete conical shells with variable thickness", *Int. J. Struct. Stab. Dyn.*, **14**(4), 1450001.
- Lal, R. and Rani, R. (2014), "Mode shapes and frequencies of radially symmetric vibrations of annular sandwich plates of variable thickness", *Acta Mechanica*, **225**(6), 1565-1580.
- Liu, M., Liu, J. and Cheng, Y. (2014), "Free vibration of a fluid loaded ring-stiffened conical shell with variable thickness", *J. Vib. Acoust.*, **136**, 051003-1- 051003-10.
- Ma, X., Jin, G., Xiong, Y. and Liu, Z. (2014), "Free and forced vibration analysis of coupled conical-cylindrical shells with arbitrary boundary conditions", *Int. J. Mech. Sci.*, **88**, 122-137.
- Madabhushi-Raman, P. and Davalos, J.F. (1996), "Static shear correction factor for laminated rectangular beams", *Compos. Part B: Eng.*, **27**(3-4), 285-293.
- Pai, P.F. and Schulz, M.J. (1999), "Shear correction factors and an energy-consistent beam theory", *Int. J. Solid. Struct.*, **36**, 1523-1540.
- Patel, B.P., Singh, S. and Nath, Y. (2008), "Postbuckling characteristics of angle-ply laminated truncated circular conical shells", *Commun. Nonlin. Sci. Numer. Simul.*, **13**(7), 1411-1430.
- Reddy, J.N. (1997), *Mechanics of Laminated Composite Plates*, CRC Press, New York.
- Selahi, E., Setoodeh, A.R. and Tahani, M. (2014), "Three-dimensional transient analysis of functionally graded truncated conical shells with variable thickness subjected to an asymmetric dynamic pressure", *Int. J. Press. Ves. Pip.*, **119**, 29-38.
- Shakouri, M. and Kouchakzadeh, M.A. (2014), "Free vibration analysis of joined conical shells: Analytical and experimental study", *Thin Wall. Struct.*, **85**, 350-358.
- Sofiyev, A.H., Omurtag, M.H. and Schnack, E. (2009), "The vibration and stability of orthotropic conical shells with non-homogeneous material properties under a hydrostatic pressure", *J. Sound Vib.*, **319**, 963-983.
- Sofiyev, A.H. (2014), "Large-amplitude vibration of non-homogeneous orthotropic composite truncated conical shell", *Compos. Part B: Eng.*, **61**, 365-374.
- Sofiyev, A.H. and Kuruoglu, N. (2014), "Combined influences of shear deformation, rotary inertia and heterogeneity on the frequencies of cross-ply laminated orthotropic cylindrical shells", *Compos. Part B: Eng.*, **66**, 500-510.
- Sofiyev, A.H. (2016), "Buckling of heterogeneous orthotropic composite conical shells under external pressures within the shear deformation theory", *Compos. Part B: Eng.*, **84**, 175-187.
- Su, Z., Jin, G. and Ye, T. (2014), "Three-dimensional vibration analysis of thick functionally graded conical, cylindrical shell and annular plate structures with arbitrary elastic restraints", *Compos. Struct.*, **118**, 432-447.
- Tornabene, F., Fantuzzi, N. and Baccocchi, M. (2014), "Free vibrations of free-form doubly-curved shells made of functionally graded materials using higher-order equivalent single layer theories", *Compos. Part B: Eng.*, **67**, 490-509.
- Tornabene, F., Fantuzzi, N., Viola, E. and Batra, R.C. (2015), "Stress and strain recovery for functionally graded free-form and doubly-curved sandwich shells using higher-order equivalent single layer theory", *Compos. Struct.*, **119**, 67-89.

- Viswanathan, K.K., Saira, J., Izliana, A.B. and Zainal, A.A. (2015), "Free vibration of anti-symmetric angle-ply laminated conical shells", *Compos. Struct.*, **122**, 488-495.
- Viswanathan, K.K. and Kim, K.S. (2008), "Free vibration of antisymmetric angle-ply laminated plates including shear deformation: spline method", *Int. J. Mech. Sci.*, **50**, 1476-1485.
- Wu, S., Qu, Y. and Hua, H. (2015), "Free vibration of laminated orthotropic conical shell on Pasternak foundation by a domain decomposition method", *J. Compos. Mater.*, **49**(1), 35-52.
- Xie, X., Jin, G., Ye, T. and Liu, Z. (2014), "Free vibration analysis of functionally graded conical shells and annular plates using the Haar wavelet method", *Appl. Acoust.*, **85**, 130-142.
- Zarouni, E., Jalilian Rad, M. and Tohidi, H. (2014), "Free vibration analysis of fiber reinforced composite conical shells resting on Pasternak-type elastic foundation using Ritz and Galerkin methods", *Int. J. Mech. Mater. Des.*, **10**(4), 421-438.
- Zhang, B., He, Y., Liu, D., Shen, L. and Lei, J. (2015), "Free vibration analysis of four-unknown shear deformable functionally graded cylindrical microshells based on the strain gradient elasticity theory", *Compos. Struct.*, **119**, 578-597.